
Numerical Study of Unsteady Viscous Hypersonic Blunt Body Flows with an Impinging Shock

G. H. Klopfer, H. C. Yee and P. Kutler

{NASA-TH-100096) NUMERICAL STUDY OF
UNSTEADY VISCOUS HYPERSONIC BLUNT BODY FLOWS
WITH AN IMPINGING SHOCK (NASA) 10 p

N88-22650

CSCL 12A

Unclas
G3/64 0142322

April 1988



National Aeronautics and
Space Administration

Numerical Study of Unsteady Viscous Hypersonic Blunt Body Flows with an Impinging Shock

G. H. Klopfer, NEAR Inc., Mountain View, California

H. C. Yee

P. Kutler, Ames Research Center, Moffett Field, California

April 1988



National Aeronautics and
Space Administration

Ames Research Center
Moffett Field, California 94035

NUMERICAL STUDY OF UNSTEADY VISCOUS HYPERSONIC BLUNT BODY FLOWS WITH AN IMPINGING SHOCK

G.H. Klopfer¹

NEAR, Inc., Mountain View, CA 94043

H.C. Yee² and P. Kutler³

NASA Ames Research Center, Moffett Field, CA 94035

Abstract

A complex two-dimensional, unsteady, viscous hypersonic shock wave interaction is numerically simulated by a high-resolution, second-order fully implicit shock-capturing scheme. The physical model consists of a non-stationary oblique shock impinging on the bow shock of a blunt body. Studies indicate that the unsteady flow patterns are slightly different from their steady counterparts. However, for the sample cases investigated the peak surface pressures for the unsteady flows seem to occur at very different impingement locations than for the steady flow cases.

Introduction

The recent development of high resolution total variation diminishing (TVD) schemes [1-3] has made it possible to accurately simulate the unsteady Navier-Stokes equations for complicated shock interactions at hypersonic Mach numbers. Such flows are of current interest in hypersonic aerodynamics. In a previous study [4] the steady viscous hypersonic blunt body flows with impinging shock waves were investigated. Some numerical simulations by other numerical methods for steady blunt body flows with impinging shocks have been reported in [5-8]. Very little work has been done for viscous unsteady shock interaction flows at hypersonic speeds, in particular, numerical simulations by implicit methods. The objective of this paper is to study the unsteady viscous hypersonic blunt body flows with non-stationary impinging shocks. The rapidly changing shock waves and shear layers that occur and interact with each other make this a difficult problem to simulate by classical numerical methods. Here a two-dimensional code consisting of an implicit second-order accurate (time and space) TVD-type algorithm is used to simulate the flow field. The scheme is based on an existing TVD algorithm [9,10] for transonic and supersonic flows which has been extended recently to hypersonic and equilibrium real gas flows [2,3]. The specific objective of the study is to determine the unsteady shock interference patterns and to compare them with the corresponding patterns for steady flows at various hypersonic Mach numbers. Another objective is to determine the transient surface pressures.

The Physical Problem

The physical problem examined is the unsteady hypersonic viscous two-dimensional blunt body flow with an impinging shock. A schematic of the computational domain of the flow field is shown in figure 1. The blunt body has a thickness of D and a nose radius of R_l . The circumferential angle, θ , is measured from the

¹Research Scientist

²Research Scientist, Computational Fluid Dynamics Branch

³Chief, Fluid Dynamics Division

symmetry line as depicted in the figure. This physical model can represent many practical applications. One example is the bow shock of a hypersonic aerodynamic vehicle interacting with the shocks of the leading edge of a wing or the cowl lip of the engine inlet. The interaction causes complicated shock-on-shock patterns in steady flows. Such steady interactions were studied in [4]. However, even under steady cruise conditions the vehicle bow shock fluctuates about some mean position, and thus the interaction is unsteady. The thickness of the cowl lip or wing is thin compared to the shock layer thickness, and even a small shock fluctuation causes a large excursion of the impinging shock in the vicinity of the inlet cowl or wing. This unsteady interaction is modeled by a non-stationary impinging shock (vehicle bow shock) moving downward with constant speed across the bow shock of the blunt body which can represent the cowl lip or wing leading edge. For steady flows, various kinds of shock interactions occur depending on the freestream conditions and impingement shock angle and location. Based on experimental data at supersonic speeds, Edney [11] has identified six different kinds of interactions labeled Type I through Type VI. For the Type IV interaction for steady flows, the peak surface pressure is many times larger than for the blunt body flow case. One motivation for the study is to see if the same type of amplification of the peak surface pressure values also occurs for the unsteady interaction.

Numerical Results

Due to space limitations, numerical results obtained for the unsteady laminar thin layer Navier-Stokes flows of a perfect gas are only summarized here. At present there are no experimental data available for the unsteady interactions to validate the numerical simulations. Therefore the unsteady results are compared to each other at different Mach numbers and to the steady state computations of reference 4 at the same Mach numbers.

Figure 2 presents the Mach contours at six instances of the diffraction process of an unsteady viscous computation. An impinging shock at an angle of 22.75° relative to the freestream moves down across the bow shock of the blunt body. The impingement shock velocity is 10% of the freestream velocity ($M_\infty = 15$). The freestream Reynolds number based on the diameter is $Re_D = 186,000$ and the freestream temperature is $T_\infty = 255.6^\circ K$. The Mach contours ranging from 0 to 15 in increments of 0.1 are shown in figure 2. The indicated times of each frame are normalized with the freestream velocity and cowl lip thickness. The surface pressure distributions for the last three instances compared with the steady-state case are given in figure 3. The first three surface pressure distributions are not given here and are similar to the steady case [4]. The most critical condition in terms of surface pressures no longer seems to occur for the Type IV shock interaction, as it does for the steady state case. Experimental data [11] indicates that the rates can be as much as 1000% (10 times) higher than for the non-interfering blunt body flow. Note that the shock impingement locations of the unsteady and steady computations do not coincide.

For the conditions used in this computation only the first five types of shock patterns identified by Edney are apparent in the sequence. Due to the unsteadiness, high Mach numbers, and high impingement shock angles the flow patterns are much more complex than those given by Edney. The corresponding Mach contours for the steady case at $M_\infty = 15$ are shown in figure 11 of reference 4. For both the steady and unsteady cases the same type of shock interference patterns occur although the unsteady sequence exhibits a much more complicated pattern within the shock layer. The separated boundary layer apparent for the unsteady Type I interaction does not appear for the steady Type I case with the same shock impingement angle. Also the supersonic jets flowing parallel to the blunt body surface and below the impingement point in the Type III and IV unsteady flows do not occur for the steady state cases. However for the Type V shock interference, where a new 2-D blunt body flow forms with the freestream conditions of those of a supersonic wedge flow, there are very little differences between the steady and unsteady flows.

The last set of results is shown in figures 4 and 5 for an unsteady Navier-Stokes computation at Mach 5.94. The freestream Reynolds number based on the diameter is $Re_D = 186,000$ and the freestream temperature is $T_\infty = 59.5^\circ K$. To demonstrate the differences at the two Mach numbers a similar sequence is used as for the Mach 15 case. For the Type I and II flows the shock patterns differ from the Mach 15 case for identical impingement shock location. However, for Type III to Type V flows, the shock patterns and locations are the same. Another notable difference at the two Mach numbers is that for the Type I flow, the transmitted shock causes the wall boundary layer to separate and thus becomes a lambda shock at the higher Mach number. The boundary layer does not separate at the lower Mach number. The boundary layer separation

has not been observed for the steady flows computed so far. The surface pressure distributions compared with the steady case are given in figure 5 for the last three of the six instances shown in figure 4. The Mach contours for the steady case can be found in figure 5 of reference 4. Similar to the Mach 15 case, the unsteady peak surface pressures no longer seem to occur for the Type IV shock interaction as they do for the steady flows.

Comparison of the computed results for the surface pressures of the steady shock interaction with the experimental data of Keyes given in [12] can be found in reference 4 and is shown in figure 5. A complete description of the steady state results for various Mach numbers is also given in reference 4, where in particular the numerical computations are compared to the various experimental data in terms of the surface pressures and heat transfer rates. The comparison serves to validate the code used for the present study.

Conclusions

Numerical simulation of the unsteady Navier-Stokes equations with a high resolution time-accurate implicit TVD scheme for predicting the complicated shock-on-shock interaction on a blunt body with a non-stationary impinging shock has been carried out. It has been demonstrated that similar types of shock interactions occur for the unsteady flows as for the steady cases identified by Edney. However, for the sample cases studied in this paper the peak surface pressures do not seem to occur during the Type IV interaction as for the steady case. The significance of this fact is that the Type III interaction occurs for a much broader range of impingement shock angles and positions than for the Type IV interaction. Also the details within the shock layer differ appreciably. For example boundary layer separation and transient supersonic jets flowing parallel to the blunt body surface occur for the unsteady but not for the steady shock interactions.

References

1. Yee, H.C.; "Upwind and Symmetric Shock-Capturing Schemes," NASA TM- 89464, May 1987.
2. Montagne, J.-L., Yee, H.C., Klopfer, G.H. and Vinokur, M.; "Hypersonic Blunt Body Computations Including Real Gas Effects," *Proceed. of the 2nd Int'l. Conf. on Hyperbolic Problems*, March 13-18, 1988, Aachen, Germany, also NASA TM-100074, March 1988.
3. Yee, H.C., Klopfer, G.H. and Montagne, J.-L.; "High Resolution Shock Capturing Schemes for Inviscid and Viscous Hypersonic Flows," *Proceed. of the BAIL V Conf.*, June 20-24, 1988, Shanghai, China, also NASA TM-100097, April 1988.
4. Klopfer, G.H. and Yee, H.C.; "Viscous Hypersonic Shock-on-Shock Interaction on Blunt Cowl Lips," AIAA Paper 88-0233, Jan. 1988.
5. Tannehill, J.C., Holst, T.L., and Rakich, J.V.; "Numerical Computation of Two-Dimensional Viscous Blunt Body Flows with an Impinging Shock," AIAA J., Vol. 14, No. 2, February 1976.
6. White, J.A., and Rhie, C.M.; "Numerical Analysis of Peak Heat Transfer Rates for Hypersonic Flow over a Cowl Leading Edge," AIAA Paper 87-1895, June 1987.
7. Rhie, C.M. and Stowers, S.T.; "Navier-Stokes Analysis for High Speed Flows Using a Pressure Correction Algorithm," AIAA Paper 87-1980, June 1987.
8. Thareja, R.R., Stewart, J.R., Hassan, O., Morgan, K., and Peraire, J.; "A Point Implicit Unstructured Grid Solver for the Euler and Navier-Stokes Equations," AIAA Paper 88-0036, January 1988.
9. Harten, A.; "On a Class of High Resolution Total Variation Stable Finite Difference Schemes," *SIAM J. Num. Anal.*, Vol 21, pp.1-23, 1984.
10. Yee, H.C.; "Linearized Form of Implicit TVD Schemes for Multidimensional Euler and Navier-Stokes Equations," *Comp. of Maths. with Appls.*, Vol. 12A, pp.413-432, 1986.
11. Edney, B.E.; "Anomalous Heat Transfer and Pressure Distributions on Blunt Bodies at Hypersonic Speeds in the Presence of an Impinging Shock," FFA Rept. 115, February 1968, The Aeronautical Research Institute of Sweden, Stockholm, Sweden.
12. Tannehill, J.C., Holst, T.L., Rakich, J.V., and Keyes, J.W.; "Comparison of a Two-Dimensional Shock Impingement Computation with Experiment," AIAA J., Vol. 14, No. 4, April 1976.

ORIGINAL PAGE IS
OF POOR QUALITY

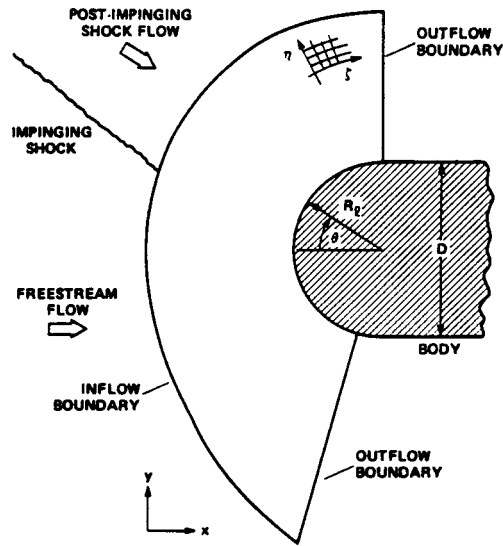


Fig. 1 Schematic of the computational domain.

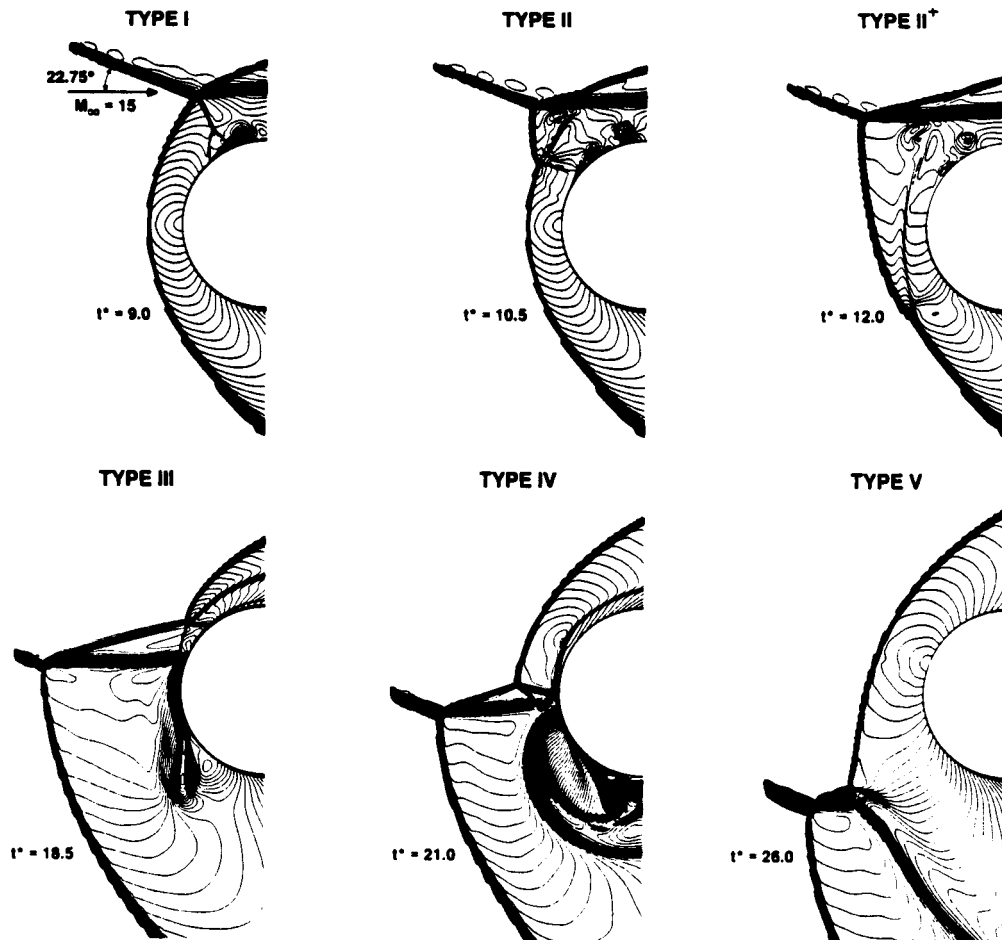
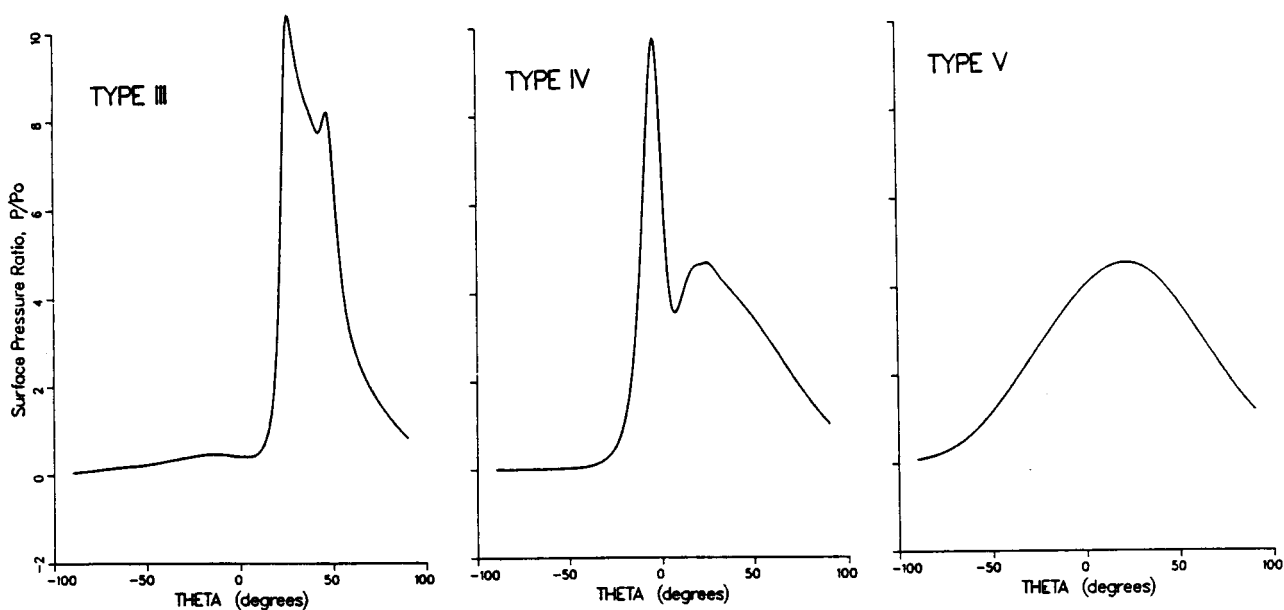
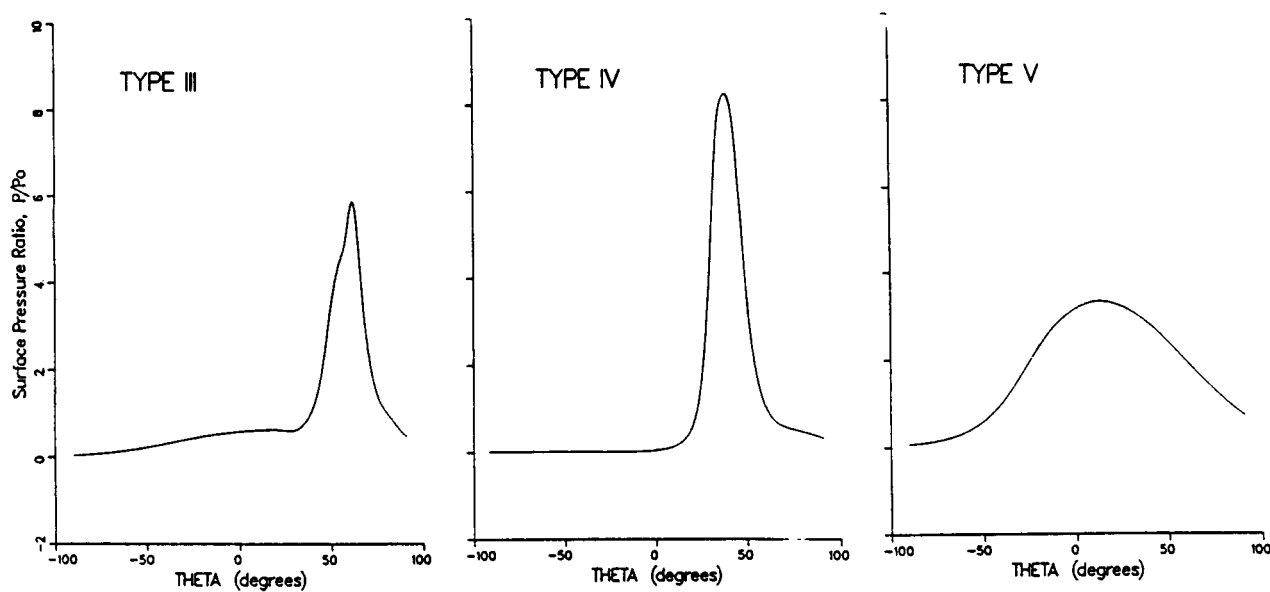


Fig. 2 Mach contours at six instances of the diffraction process with $M_\infty = 15$ and $Re_D = 186,000$. The indicated times (t^*) of each frame are normalized with the freestream velocity and blunt body thickness.



(a) unsteady



(b) steady

Fig. 3 The surface pressure distributions for Types III, IV, and V shock interactions at $M_\infty = 15$. The unsteady sequence is for the last three instances shown in figure 2. The steady sequence is for the last three views shown in figure 11 of reference [4].

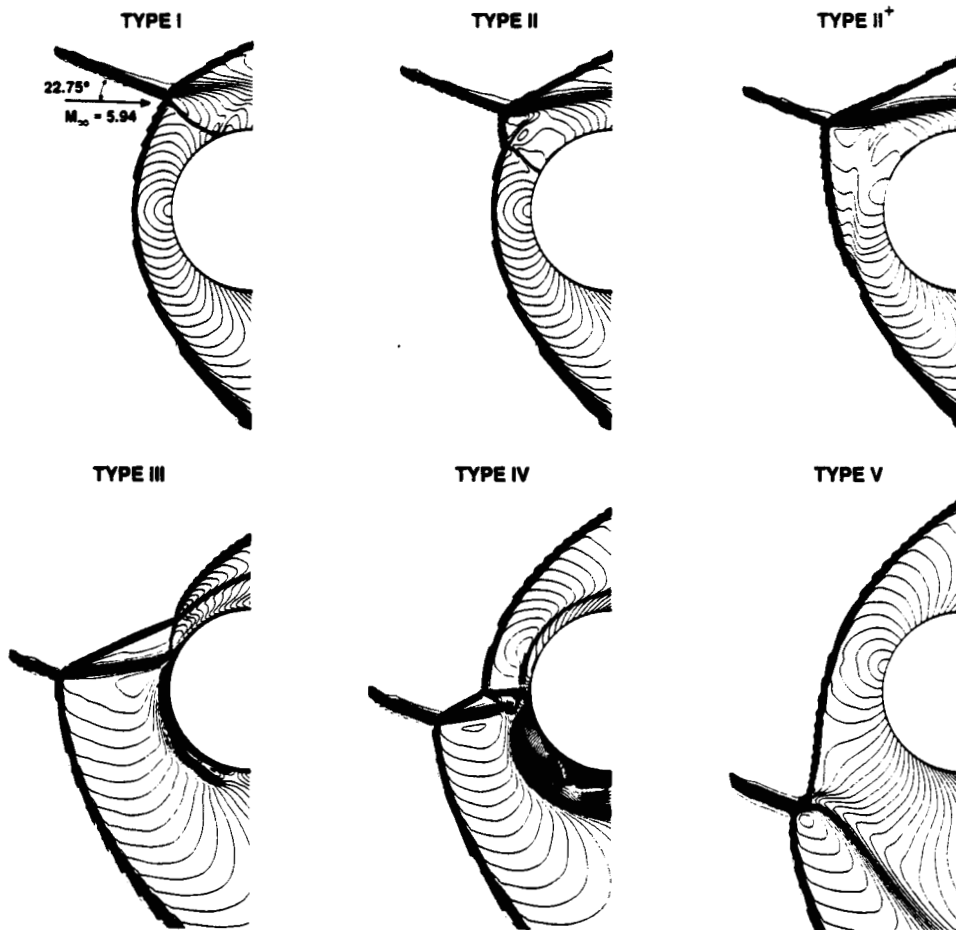
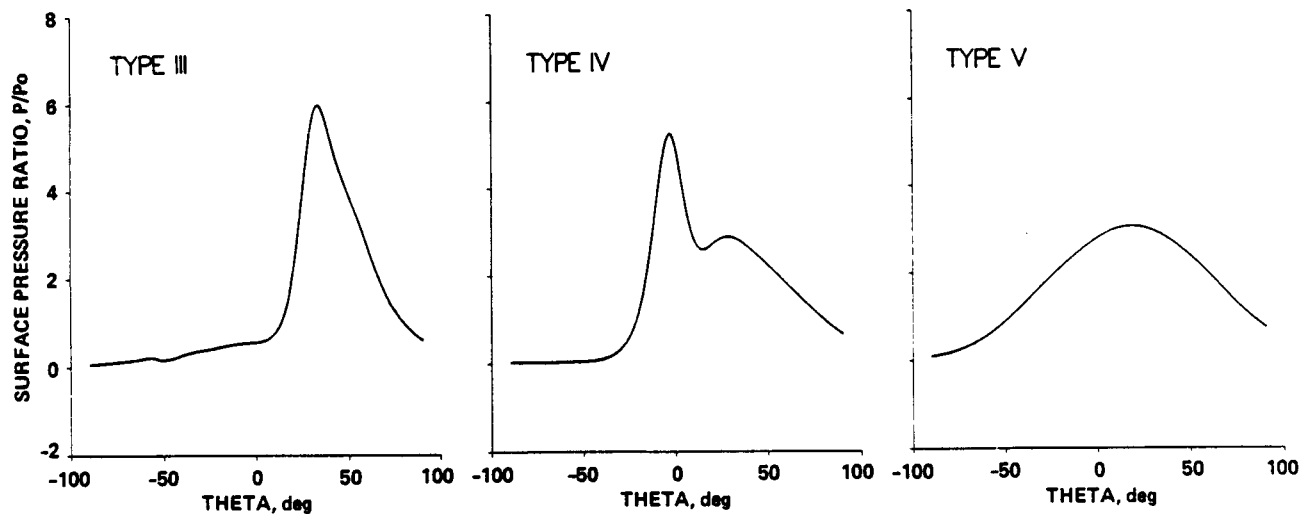
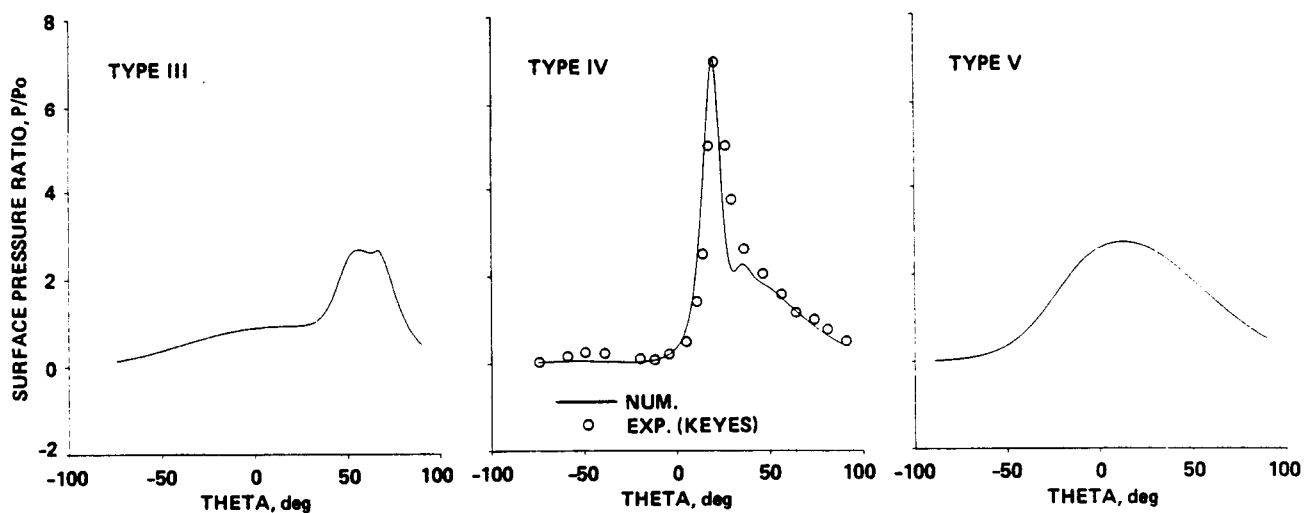


Fig. 4 Mach contours at six instances of the diffraction process with $M_\infty = 5.94$ and $Re_D = 186,000$. Same types of shock-on-shock interference as shown in figure 2.



(a) unsteady



(b) steady

Fig. 5 The surface pressure distributions for Types III, IV, and V shock interactions at $M_\infty = 5.94$. The unsteady sequence is for the last three instances shown in figure 4. The steady sequence is for the last three views shown in figure 5 of reference [4].



Report Documentation Page

1. Report No. NASA TM-100096		2. Government Accession No.		3. Recipient's Catalog No.	
4. Title and Subtitle Numerical Study of Unsteady Viscous Hypersonic Blunt Body Flows with an Impinging Shock				5. Report Date April 1988	
				6. Performing Organization Code	
7. Author(s) G. H. Klopfer, H. C. Yee, and P. Kutler				8. Performing Organization Report No. A-88147	
				10. Work Unit No. 505-60	
9. Performing Organization Name and Address Ames Research Center Moffett Field, CA 94035				11. Contract or Grant No.	
				13. Type of Report and Period Covered Technical Memorandum	
12. Sponsoring Agency Name and Address National Aeronautics and Space Administration Washington, DC 20546-0001				14. Sponsoring Agency Code	
15. Supplementary Notes Point of Contact: Helen C. Yee, Ames Research Center, MS 202A-1, Moffett Field, CA 94035 (415) 694-4769 or FTS 464-4769					
16. Abstract A complex two-dimensional, unsteady, viscous hypersonic shock wave interaction is numerically simulated by a high-resolution, second-order fully implicit shock-capturing scheme. The physical model consists of a non-stationary oblique shock impinging on the bow shock of a blunt body. Studies indicated that the unsteady flow patterns are slightly different from their steady counterparts. However, for the sample cases investigated the peak surface pressures for the unsteady flows seem to occur at very different impingement locations than for the steady flow cases.					
17. Key Words (Suggested by Author(s)) Unsteady viscous flows Hypersonic flows Blunt body flows with an impinging shock Numerical simulations				18. Distribution Statement Unclassified-Unlimited Subject Category - 64	
19. Security Classif. (of this report) Unclassified		20. Security Classif. (of this page) Unclassified		21. No. of pages 8	
				22. Price A02	